

## HUBBLE SPACE TELESCOPE OBSERVATIONS OF THE INTERACTING GALAXIES NGC 2207 AND IC 2163<sup>1</sup>

BRUCE G. ELMEGREEN,<sup>2</sup> MICHELE KAUFMAN,<sup>3</sup> CURTIS STRUCK,<sup>4</sup> DEBRA MELOY ELMEGREEN,<sup>5</sup> ELIAS BRINKS,<sup>6</sup>  
MAGNUS THOMASSON,<sup>7</sup> MARIO KLARIĆ,<sup>8</sup> ZOLT LEVAY,<sup>9</sup> JAYANNE ENGLISH,<sup>9</sup> L. M. FRATTARE,<sup>9</sup>  
HOWARD E. BOND,<sup>9</sup> C. A. CHRISTIAN,<sup>9</sup> F. HAMILTON,<sup>9</sup> AND K. NOLL<sup>9</sup>

Received 2000 February 25; accepted 2000 May 2

### ABSTRACT

*Hubble Space Telescope (HST)* images of the galaxies NGC 2207 and IC 2163 show star formation and dust structures in a system that has experienced a recent grazing encounter. Tidal forces from NGC 2207 compressed and elongated the disk of IC 2163, forming an oval ridge of star formation along a caustic where the perturbed gas rebounded after its inward excursion. Gas flowing away from this ridge has a peculiar structure characterized by thin parallel dust filaments transverse to the direction of motion. The filaments become thicker and longer as the gas approaches the tidal arm. Star formation that occurs in the filaments consistently lags behind, as if the exponential disk pressure gradient pushes outward on the gas but not on the young stars. Numerical models suggest that the filaments come from flocculent spiral arms that were present before the interaction. The arms stretch out into parallel filaments as the tidal tail forms. A dust lane at the outer edge of the tidal tail is a shock front where the flow abruptly changes direction. Gas at small-to-intermediate radii along this edge flows back toward the galaxy, while elsewhere in the tidal arm, the gas flows outward.

A spiral arm of NGC 2207 that is backlit by IC 2163 is seen with *HST* to contain several parallel, knotty filaments spanning the full width of the arm. These filaments are probably shock fronts in a density wave. The parallel structure suggests that the shocks occur in several places throughout the arm, or that the interarm gas is composed of spiral-like wisps that merge together in the arms. Blue clusters of star formation inside the clumps of these dust lanes show density-wave triggering in unprecedented detail. The star formation process seems to be one of local gravitational collapse, rather than cloud collisions. Spiral arms inside the oval of IC 2163 have a familiar geometry reminiscent of a bar, although there is no obvious stellar bar. The shape and orientation of these arms suggest they could be the result of inner Lindblad resonance-related orbits in the  $\cos 2\theta$  tidal potential that formed the oval. Their presence suggests that tidal forces alone may initiate a temporary nuclear gas flow and eventual starburst without first forming a stellar bar. Several emission structures resembling jets or conical flows that are 100–1000 pc long appear in these galaxies. In the western arm of NGC 2207, there is a dense dark cloud with a conical shape 400 pc long and a bright compact cluster at the tip, and there is a conical emission nebula of the same length that points away from the cluster in the other direction. This region also coincides with a nonthermal radio continuum source that is  $\sim 1000$  times the luminosity of Cas A at  $\lambda = 20$  cm. Surrounding clusters in arclike patterns may have been triggered by enormous explosions.

*Key words:* dust, extinction — galaxies: interactions — galaxies: ISM — ISM: jets and outflows — ISM: kinematics and dynamics

### 1. INTRODUCTION

The spiral galaxies IC 2163 and NGC 2207 are currently involved in a near-grazing encounter (Elmegreen et al. 1995b, 1995a, hereafter Papers III and IV, respectively). Tidal forces distorted IC 2163 in the in-plane direction, forming a tidal arm with two velocity components on the anticompanion side, and forming an intrinsically oval disk with an eye-shaped (“ocular”) morphology. Streaming motions in the oval are in excess of  $100 \text{ km s}^{-1}$ . Tidal forces also distorted NGC 2207 perpendicular to the plane, forming a strong, twisting warp. The H I in both galaxies has a large velocity dispersion of  $30\text{--}50 \text{ km s}^{-1}$  and is concentrated in unusually large clouds ( $10^8 M_{\odot}$ ; Elmegreen, Kaufman, & Thomasson 1993, hereafter Paper II). Numerical simulations reproduced these peculiar structures and internal velocities with a prograde encounter affecting IC

<sup>1</sup> Based on observations with the NASA/ESA *Hubble Space Telescope*, obtained at the Space Telescope Science Institute, which is operated by the Association of Universities for Research in Astronomy, Inc., under NASA contract NAS 5-26555.

<sup>2</sup> IBM Research Division, T. J. Watson Research Center, P.O. Box 218, Yorktown Heights, NY 10598; bge@watson.ibm.com.

<sup>3</sup> Department of Physics and Department of Astronomy, Ohio State University, 174 West 18th Avenue, Columbus, OH 43210; rallis@mps.ohio-state.edu.

<sup>4</sup> Department of Physics and Astronomy, Iowa State University, Ames, IA 50010-3160; curt@iastate.edu.

<sup>5</sup> Department of Physics and Astronomy, Vassar College, Poughkeepsie, NY 12604; elmegreen@vassar.edu.

<sup>6</sup> Departamento de Astronomía, Universidad de Guanajuato, Apdo. Postal 144, 36000 Guanajuato, Gto., Mexico; ebrinks@astro.ugto.mx.

<sup>7</sup> Onsala Space Observatory, S-439 92 Onsala, Sweden; magnus@oso.chalmers.se.

<sup>8</sup> 5821 Satchelford Road, Columbia, SC 29206; mariok@cris.com.

<sup>9</sup> Space Telescope Science Institute, 3700 San Martin Drive, Baltimore, MD 21218.

2163 and a perpendicular encounter affecting NGC 2207 (Paper IV). The closest approach was around 40 Myr ago at a separation of only about two radii. This makes IC 2163 and NGC 2207 ideal for studying close encounters between galaxies and how they might trigger bars or starbursts.

Three systems of interacting galaxies (IC 2163, NGC 2535, and NGC 5394) have now been studied by our group to see how structures resulting from prograde, in-plane, nearly grazing encounters evolve in time (Papers III, IV; Kaufman et al. 1997, 1999). IC 2163 is the interaction that is least evolved. In all three cases, the prograde galaxy has two long tidal arms with a large arm-interarm contrast, misalignment between the kinematic and photometric axes indicative of an intrinsically oval disk, and widespread high velocity dispersions in the H I gas. NGC 2535 is an ocular galaxy, but unlike IC 2163, it has no enhanced H I or radio continuum emission on the rim of the oval; this indicates that it is in a later phase than IC 2163 (Elmegreen et al. 1991, hereafter Paper I). There is also evidence for mass transfer from NGC 2535 to its small starburst companion. NGC 5394 has no ocular structure but bright spiral arms in the inner disk and a nuclear starburst, making it more evolved than NGC 2535.

To study these grazing encounters in more detail, we observed the IC 2163/NGC 2207 pair with the Wide Field Planetary Camera 2 (WFPC2) on the *Hubble Space Telescope* (*HST*) in 1996 May and 1998 November. Based on these observations, this paper describes (1) an improved understanding of the formation mechanism of the tidal tail in IC 2163, with a detailed numerical simulation of the gas (§§ 4.1 and 4.2); (2) a new view of the density-wave structure and star formation in a spiral arm, as seen in a backlit portion of NGC 2207 (§ 4.3); (3) bright star formation associated with a strong nonthermal radio source on an outer spiral arm (§ 5); (4) the possibility that interactions can induce transient nuclear gas inflow via barlike hydrodynamics, even if a genuine bar is absent (§ 6); (5) peculiar jetlike or curved emission features (§ 7); and (6) the H I–star formation connection (§ 8). Other studies of the star-forming regions and dust opacities will be reported elsewhere (Elmegreen et al. 2000b, hereafter Paper V; see also Berlind et al. 1997). The *HST* observations also revealed peculiar dust spirals in the nucleus of NGC 2207; these were analyzed in terms of acoustic instabilities in Elmegreen et al. (1998).

## 2. OBSERVATIONS AND DATA REDUCTION

The galaxies IC 2163 and NGC 2207 were observed in nine orbits with the *HST* WFPC2 using filters F336W (*U* band), F439W (*B* band), F555W (*V* band), and F814W (*I* band). Four exposures in each band concentrated on a field in the northwest, and four more exposures of each of two fields were made for the central and eastern parts. The images were dithered between each exposure, and the exposure times were 500 s in *U*, 500 s in *B*, 160 s in *V*, and 180 s in *I*. The average scale is  $0''.0995 \text{ pixel}^{-1}$  for the wide-field images and  $0''.0455 \text{ pixel}^{-1}$  for the Planetary Camera (PC) images.

From these 48 individual pipeline-processed exposures (four filters, three pointings, two dither positions per pointing, and two CR-SPLITS per position), cosmic-ray split pairs were combined for each dither position chip by chip. Individual WFPC2 chips were then combined for each dither position into  $2907 \times 1486$  pixel mosaics. The dither

positions were registered and combined, resulting in a single image for each filter and pointing (12 images). A three-color composite image was produced (using IDL) for each pointing, and the three pointings were registered and mosaicked (using Adobe Photoshop) into a single image. The initial step in creating each three-color image involved clipping and logarithmically scaling the intensities in each filter. Then each filter was assigned, in chromatic order, to a color channel: red =  $\log I$ , green =  $\log V$ , blue =  $\log(B + U)$ . The three channels of the mosaicked image were combined using the “screen” algorithm in Photoshop. The channels were adjusted in order to match more closely the visual color of the central wavelength of each filter. This produced an overall bright image with a neutral color background, and it increased the intensity and color dynamic ranges in order to emphasize individual features. The noisier PC chip was Gaussian smoothed to match the texture of the other chips. Finally, the remaining artifacts (hot pixels, chip seams, etc.) were removed using Photoshop.

For comparison with H I and radio continuum images, a *B*-band mosaic was transformed to right ascension and declination coordinates. The uncertainty in the registration to absolute coordinates is about  $\pm 0''.8$ , partly as a result of uncertainties in the positions of the guide stars and secondary standard stars and partly as a result of the standard deviations of the plate solution. The *B*-band mosaic in absolute coordinates was rotated  $10^\circ.7$  counterclockwise relative to the color mosaic displayed in Figure 1 below.

## 3. BASIC MORPHOLOGY OF THE INTERACTING GALAXIES

A mosaic of three *HST* WFPC2 pointings of the galaxy pair IC 2163/NGC 2207 is shown in Figure 1, with north up relative to the figure legend. A digitized version of this figure may be found at the Hubble Heritage World Wide Web site.<sup>10</sup> Here we comment on several unusual features. The relevant parameters for these galaxies are listed in Table 1. At the distance of 35 Mpc ( $H_0 = 75 \text{ km s}^{-1} \text{ Mpc}^{-1}$ ),  $1''$  corresponds to 170 pc.

The morphology, interaction dynamics, and orbital history of this system were discussed, along with numerical simulations of each galaxy, in Papers III and IV. These previous simulations considered stars only, without gas. This was enough to get the basic disk structure. A new simulation of the tidal arm discussed below includes gas. The orbit that we fitted previously had the smaller galaxy, IC 2163 (presently in the east), pass from the near side of NGC 2207 to the far side several hundred million years ago, at a point in the west about two NGC 2207 radii away from the center of NGC 2207. IC 2163 then moved behind NGC 2207 in an easterly direction, passing perigalacticon at a distance of about two of its own radii some 40 Myr ago. IC 2163 is currently moving southeasterly. These relative distances are uncertain because they depend on the size and mass of the halo around each galaxy. The orbit is constrained by the internal structures and velocities of the galaxies, by their similar line-of-sight velocities (which implies that they are presently moving nearly parallel to each other in the sky plane), and by the extended pool of optical and H I emission that lies south of NGC 2207. This pool seems to be the point of the previous disk crossing, where IC 2163

<sup>10</sup> See <http://heritage.stsci.edu>.



FIG. 1.—Interacting galaxies IC 2163 (*left*) and NGC 2207 (*right*), from a mosaic of three *HST* pointings. North is up.

TABLE 1  
BASIC DATA ON IC 2163/NGC 2207

Characteristic	IC 2163	NGC 2207
Morphological type .....	SB(rs)c pec	SAB(rs)bc pec
R.A. (B1950.0) .....	6 14 20.0	6 <sup>h</sup> 14 <sup>m</sup> 14 <sup>s</sup> .4
Decl. (B1950.0) .....	-21 21 24	-21°21'14"
R.A. (J2000.0) .....	6 16 27.7	6 <sup>h</sup> 16 <sup>m</sup> 27 <sup>s</sup> .1
Decl. (J2000.0) .....	-21 22 21	-21°22'21"
Isophotal major radius, $R_{25}$ (arcmin).....	1.51	2.13
Axis ratio .....	2.45	1.55
$m_B$ .....	12.55	11.59
Corrected $B$ magnitude, $B_T^0$ .....	11.26	10.90
Distance (Mpc) .....		35
Velocity ( $\text{km s}^{-1}$ ) .....	$2765 \pm 20$	$2745 \pm 15$

NOTE.—Units of right ascension are hours, minutes, and seconds, and units of declination are degrees, arcminutes, and arcseconds.

passed through the outer disk plane of NGC 2207, now rotated clockwise by about one-quarter revolution.

During this interaction, IC 2163 experienced the tidal force from NGC 2207 in a prograde, in-plane direction, and subsequently developed an ocular, or oval-like, caustic structure midway out in the disk. Such ocular structure is the result of a rapid inward motion of both stars and gas in the disk of IC 2163, initiated by the stretching and compressing action of the tidal force and amplified by self-gravity in the disk of IC 2163 (Sundin 1989; Paper I; Donner, Engström, & Sundelius 1991). The inward motion causes an azimuthal speed-up in the counterclockwise direction, and the radial motion then bounces because of angular momentum conservation. The oval marks the inner extent of this radial excursion. The minor kinematic axis of IC 2163 lies  $\sim 117^\circ$  away from the minor photometric axis, indicating an intrinsically oval disk.

There is a peculiar streaming motion along the oval of about  $65 \text{ km s}^{-1}$  counterclockwise (Paper III). The line-of-sight component of the peculiar velocity increases to  $\sim 150 \text{ km s}^{-1}$  as the H I gas and stars enter the tidal arm from the northwest, and then it decreases suddenly to less than  $50 \text{ km s}^{-1}$  toward the outer edge of the tidal arm (Fig. 10 of Paper III). This motion was evident in the channel maps of Paper III (Fig. 4) and in a velocity-position map (Fig. 9), but in the line-integrated velocity map the streaming motion was less obvious. Nevertheless, in the velocity field image in Paper III (Fig. 11), the highest velocity gas occurs at the eastern end of the northern eyelid, displaced  $63^\circ$  in position angle from the kinematic minor axis rather than  $90^\circ$  for a normal rotation curve.

In Paper III we referred to the eastern tip of the oval, where the noncircular motion peaks, as the launch point for gas leaving the caustic and entering the tidal arm. The gas streams outward here mainly because it is traveling too fast for a circular orbit, but tidal forces also produce some outward acceleration. By the time the gas reaches the southern edge of the tidal arm, its peculiar motion has slowed down because of the gravity of the galaxy and large-scale shocks.

During the formation of the tidal tail in IC 2163, NGC 2207 experienced a perpendicular tidal forcing from the gravity of IC 2163. This perturbation seems to have created an inward-propagating tidal warp with an overall spiral shape, as determined by shear and disk self-gravity (Paper IV). The corresponding warp in the velocity field was clearly

seen (Paper III), although the optical disk shows little evidence of it. The warp is such that the side of NGC 2207 closest to IC 2163 in projection is warped toward it by about 9 kpc compared with the average inner disk plane.

#### 4. PECULIAR DUST STRUCTURES

Dust features are sensitive indicators of shock fronts because even small compressions can change the gas from optically thin to optically thick. There are many interesting dust structures in these galaxies as a result of the complex and unusual dynamics of the interstellar media. The high resolution and the backlighting of the outer spiral arm of NGC 2207 by IC 2163 provide a unique opportunity to study these structures.

Two peculiar dusty regions will be highlighted here: the parallel striations in the tidal tail of IC 2163, and the foreground spiral arms in NGC 2207. A dense dark cloud in the far western arm of NGC 2207 will be considered in the next section.

##### 4.1. Parallel Dust Filaments in the Tidal Tail of IC 2163

The tidal tail in IC 2163 begins at the eastern end of the inner oval with a broad and shallow distribution of starlight. Gas and stars flow outward and downward, ending abruptly in the southeast along a curving arc where there is a dust lane, and extending northwest along the length of the arm for  $\sim 15 \text{ kpc}$ . A dwarf galaxy with unknown velocity lies just off the tip of the tidal arm (the presence of globular clusters around this nucleated dwarf elliptical suggests it is not related to the interaction; see Paper V). Along the tidal outflow, there are numerous, nearly parallel dust filaments perpendicular to the flow direction  $\sim 0''.5 = 85 \text{ pc}$  thick, spaced by about  $2''$ . The filaments are darker than the surrounding regions by 0.2–0.8 mag in  $V$  band, suggesting that the midplane densities are enhanced by a factor of  $\sim 5$  compared with the interfilament gas (Paper V). The filament widths increase toward the outer edge of the tidal arm, where they take the form of two long, dense dust lanes, still parallel to each other. There is a slight tendency for the highest opacity dust streamers to occur at smaller radii (Paper V).

In our previous simulations considering only stars (Paper IV), the broad plateau of light on the inside part of the eastern tidal arm is a region of outward-streaming stars. The outward motion is  $150 \text{ km s}^{-1}$  in places and is the result of angular momentum conservation correcting for the inward plunge that these same stars recently made in response to the tidal force and self-gravity (Papers I and IV). The stars stream outward and form the tidal arm, where they slow down to a lower streaming speed of  $50 \text{ km s}^{-1}$ . These model velocities for stars were chosen to match the observed velocities for the gas. Ground-based observations could barely resolve the dense, double dust lane at the edge of the arm, and they could not see the fainter filaments in the broad plateau.

Paper III briefly considered the possibility that the split in the tidal arm of IC 2163 was the result of dust, but we favored a different interpretation in which it resulted from two separate stellar arms created for a short time during the interaction. One of these arms was a caustic, reproduced by the model, and the other was a normal tidal arm. Now we see with higher resolution that the split is from dust and conclude that either there was no caustic arm or the present epoch is not the correct one for viewing such a short-lived

feature. The two dust lanes are hydrodynamic features, probably shock fronts, and could not be modeled before with our pure-stellar code. Thus, we performed a new model with gas.

This new model is for a nearly in-plane, prograde interaction ( $25^\circ$  inclination) between a gaseous disk galaxy and a point source. The tidal arm part of the model is shown in Figure 2. The ocular structure (i.e., the caustic oval in the inner disk) is produced again because this is a general property of prograde, nearly in-plane encounters. Here we highlight the parallel filaments in the outward-streaming regions of the tidal arm, which resemble the filamentary dust structures in Figure 1. A more detailed model of the whole two-galaxy system, including a fuller analysis of the gas motions between the galaxies and the warp in NGC 2207, will be deferred to a later paper. The filamentary arms in the tidal tail of IC 2163 are present in the detailed study too.

In the present model, the gravitational potential of IC 2163 is dominated by a dark matter halo that is effectively

rigid over the relatively short duration of this interaction. Smoothed particle hydrodynamics (Struck 1997; Kaufman et al. 1999) with 18,000 particles calculates the dynamics in the disk, which is assumed to be pure gas, using an adiabatic equation of state with heating and cooling. The initial disk was in rotational equilibrium with small thermal motions. It had an exponential density distribution over 4 scale lengths, and a thickness perpendicular to the plane equal to 1 scale length. The thermal terms lead to the formation of a multiphase initial gas. The companion is assumed to be a pure halo with half the scale length of the IC 2163 halo and 1.25 times the total IC 2163 mass. The observed ratio of  $H$ - and  $K$ -band luminosities is 1.6 (Kaufman et al. 1997).

Figure 2 shows three face-on views of the model disk and a projected view: the top left panel is the map of model points at the beginning of the interaction, using color to represent initial variations in the particle positions with galactocentric radius; the top right panel is the point map at a time representative of the current NGC 2207/IC 2163

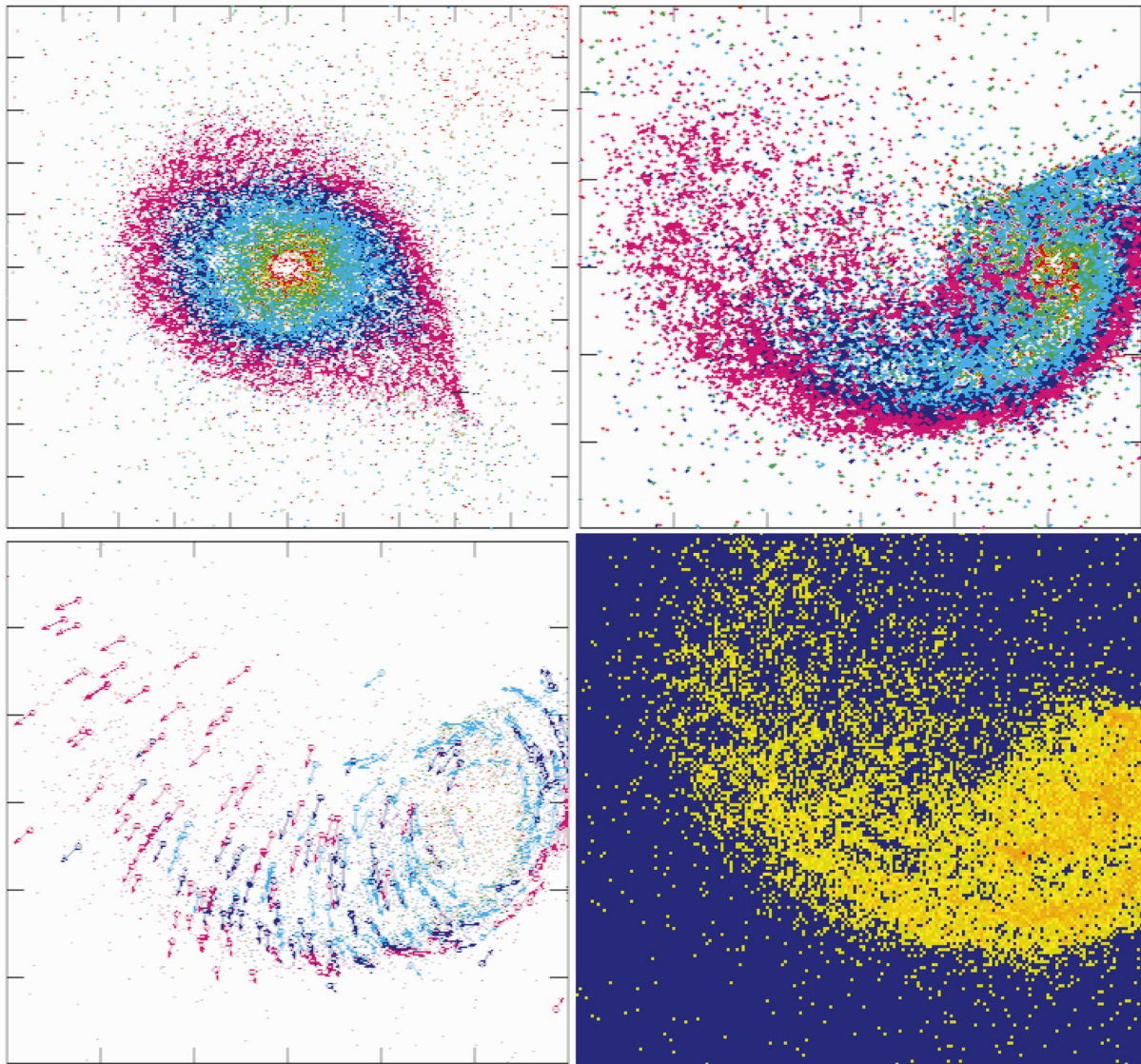


FIG. 2.—Numerical models of the parallel filaments in the tidal arm of IC 2163 at the beginning of the interaction (*top left*) and at the time best representing the current epoch (*top right*), velocity vectors at the current epoch (*bottom left*), and a projected view of the density for comparison with the image of IC 2163 in the sky, rendered as an  $160 \times 160$  array of pixels (*bottom right*). In the top and left panels, color represents initial position in the disk; in the bottom right, color represents density, going from blue to red with increasing density.

system, with the same color scheme; the bottom left shows the velocity vectors at the same time as in the top right; and the bottom right panel shows the density at the same time again, but rendered from a  $160 \times 160$  array with color proportional to the density of the model points inside each pixel (blue is low density and red is high density), and projected by an inclination of  $30^\circ$  to resemble IC 2163 in the sky. The center of the companion, NGC 2207, is off the figure in the bottom and right panels.

The tidal tail in the model has the same shape as the observed tidal tail, and an intricate network of parallel filaments is in the broad part of this tail (seen best in the bottom right panel). These filaments are stretched flocculent spiral arms that were present in the disk before perigalacticon (cf. Fig. 2, *top left*). The model generates only flocculent spirals because of the relatively high mass of the halo and the low temperature of the pure gas disk (see Elmegreen & Thomasson 1993).

The velocity vectors in the bottom left panel of Figure 2 indicate there is a shock front along the outer edge of the tidal arm, where the velocities abruptly change. This front also corresponds to a region of enhanced density, and it is located at the same place as the dense dust lane in the tidal arm of IC 2163. This result indicates that the dust lane running along the edge of the IC 2163 tidal arm is a shock front where the velocities change from outward to inward streaming. Not all of the tidal arm material is unbound from the galaxy: the inner portion returns to orbit the main disk after it shocks in the dust lane.

In Figure 1, many of the filaments in the tidal arm of IC 2163 have bright star clusters adjacent to them. These clusters are typically on the inside edges, toward smaller galactocentric radii. This is true for the small and faint dust filaments, as well as the dense dust lanes near the edge. The systematic displacement of the star clusters relative to the tidal arm dust filaments is an important check on the dynamics of the gas. Presumably, these clusters formed in the dust lanes and then became ballistic after they formed. The dust and gas are not ballistic, however, and respond to the pressure forces. Thus the relative displacement of the dust and the clusters indicates the direction of the pressure gradient. To get the dust filaments systematically outside the clusters, the gas pressure must be decreasing with increasing galactocentric radius, as expected for an exponential disk.

The displacement between stars and dust in this interpretation is unlike the situation in an idealized spiral arm shock. There the displacement inside corotation (where the stars are systematically outside the dust lanes) is the result of a spiral wave and associated shock front (the dust lanes) that move slower in the azimuthal direction than *both* the gas and the stars. The dust lane in a normal spiral is newly shocked material that did not yet form stars, while the stars and the gas clouds in which they formed are both ballistic particles that move “downstream.” The dust lane material has just been shocked and so is moving at its most negative radial speed. It is also at its largest galactocentric radius, having just streamed outward through the interarm region. As the dust lane gas moves inward and along the arm, it presumably forms clouds and stars that feel a Coriolis force deflecting them outward. In this way, their inward motion is converted into an azimuthal motion, and the young stars begin to emerge from the region of the shock toward the interarm region. For this normal spiral arm, the stars and

the dust lane are displaced from each other because these two features are at different parts of their epicycles: the dust lanes are where the radial motion is greatest inward and the azimuthal motion relatively small, while the stars and associated clouds just downstream from the dust lanes are entering the parts of their epicycles where the azimuthal motion is greatest in the prograde sense. This juxtaposition creates the illusion that the stars formed out of gas that is located in the dust lane right next to them, but this is not the case. Instead, the young stars formed in gas clouds that are moving downstream with them, and the dust lane next to these stars is newly shocked material that has just arrived in the wave. The process of star formation in spiral arms will be discussed further in § 4.3.

For the dust lanes in the tidal tail of IC 2163, the situation should be different. This is a stretched and distorted part of the former galaxy, and the motions through the arm are largely radial. In this case, the radial disk gradient of the interstellar pressure contributes to the force on the gas, pushing it faster than the stars that recently formed.

#### 4.2. Comparison between the Dust and Atomic Hydrogen in the Tidal Arm of IC 2163

Papers III and IV found H I streaming motions in the tidal arm of IC 2163 that are consistent with the outward flow of gas expected from the arm formation models. Figure 3 shows the H I overlaid on the *B*-band *HST* image. The triangles correspond to the ridge of maximum streaming speed, where the line-of-sight velocity is fairly constant at  $2970\text{--}2990 \text{ km s}^{-1}$  (the galaxy systemic velocity is  $2765 \pm 20 \text{ km s}^{-1}$ ). The pentagons correspond to a ridge of lower speed, ranging from  $2780$  to  $2930 \text{ km s}^{-1}$  (Paper III, § 4.2). The plus signs are along the dividing line between the high-velocity and the low-velocity H I ridges, where the H I intensity is low.

In Paper III, we expected the dividing line to lie at a dust lane, where the high-speed stream suddenly shocked into the low-speed gas and the H I was converted into  $\text{H}_2$ . This does not appear to be the case. Instead, the streaming ridge corresponds to a diffuse, optically faint region on the northern part of the tidal arm, and the low-speed gas in the south corresponds to the unresolved combination of the two main dust filaments. The dividing line (Fig. 3, *plus signs*) is unrelated to the main dust lanes because it has a different curvature. The H I arm also has an S-shaped wiggle at  $\alpha = 6^{\text{h}}14^{\text{m}}25^{\text{s}}\text{--}6^{\text{h}}14^{\text{m}}27^{\text{s}}$  (B1950.0), where the high- and low-velocity components of the arm appear to merge. The dust lanes do not show this structure.

The new model in Figure 2 explains the origin of these moving streams. Most of the high-velocity stream in the northern part of the tidal arm is from the original outer disk of IC 2163, which was H I dominated and had a low stellar density before the encounter. The optical faintness of the northern part of the arm is consistent with an outer disk origin. The H I gas in this region moves quickly on its way to the tip of the arm, where it may form a large gas pool (cf. Paper II). The intermediate zone of low H I emission (*plus signs*) is mostly stellar, and it comes from the intermediate-to-outer radii of the optical disk of the former IC 2163. This part of the tidal tail moves in a southeasterly direction through the arm at a steady projected speed until the gas shocks along the curved arm edge. Then it forms the prominent parallel dust lanes at a relatively low line-of-sight velocity, corresponding to some of the gas moving inward.

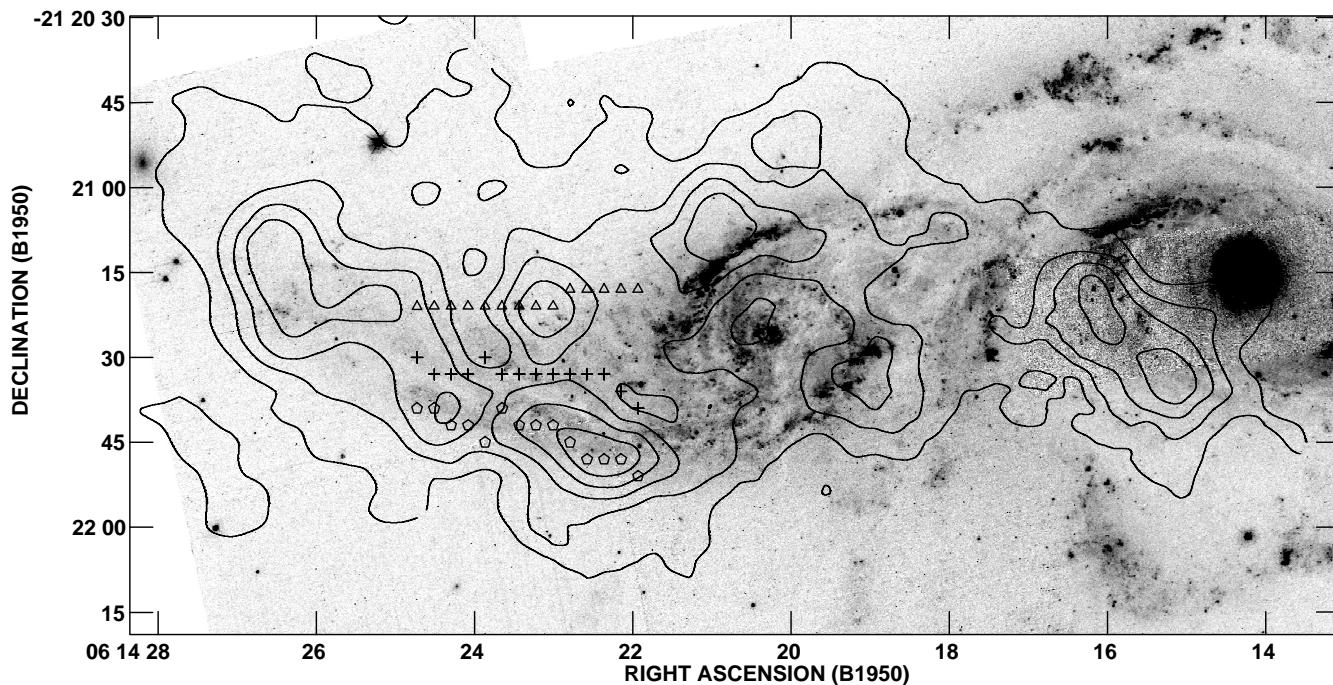


FIG. 3.—H I column density contours of IC 2163 (from Paper III) with a resolution of  $13''.5 \times 12''$  (FWHM) overlaid on the *HST* *B*-band image in gray scale. Contour levels of the line-of-sight H I column density are 5, 10, 15, 20, and  $25 M_{\odot} \text{pc}^{-2}$ . On the eastern side of IC 2163, triangles on the tidal tail mark the ridge of the high-velocity H I streaming component, pentagons mark the ridge of the low-velocity H I component, and plus signs mark the dividing line between the high- and low-velocity H I ridges. On the western side of IC 2163, there appears to be a faint blue arm coincident with the H I tidal bridge.

The asymmetry in the falloff of the H I intensity on the northern and southern sides of the tidal arm is consistent with this picture: the northern H I is extended gas that may have come all the way from the companion side of the IC 2163 outer disk, whereas the southern H I is mostly shocked gas at the leading front of the tidal arm. Figure 3b of the model in Paper II illustrates this morphology.

#### 4.3. Foreground Dust in the NGC 2207 Spiral Arms

The background lighting by IC 2163 provides a unique view of the dust lane and star formation in an outer spiral arm of NGC 2207. What appears in a ground-based image to be a single dust lane in a spiral arm of NGC 2207 is seen at higher resolution to consist of four to seven nearly parallel dust streamers that span the full width of the arm. The *V*-band magnitude decrements in many of the dust features of these arms are in the range from 0.4 to 1.5 mag (Paper V).

The spiral arm dust lanes in the *HST* image of NGC 2207 show an intricate internal structure reminiscent of Galactic cirrus clouds (Low et al. 1984) or other diffuse interstellar structures in the Milky Way, but on a much larger scale. There are also blue stars or clusters adjacent to many of the dust clouds, as if they just formed there. These spiral arms are density waves in NGC 2207, and their dust structures presumably delineate the shocks in these arms, as in the standard theory (Roberts 1969). However, the shocks are not smooth, and they are not just clumpy in the usual sense either (e.g., Combes & Gerin 1985; Roberts & Stewart 1987; Elmegreen 1988). They are mostly composed of long, knotty filaments, which in some places run side by side in parallel streaks. Such structure suggests that the density-wave shock occurred in several separate places along the width of the arm, or that the interarm gas is not in the form of spherical clouds, but filamentary as in M51 (Block et al. 1997).

We do not see the old stars in these arms, because they are too faint compared with the background disk of IC 2163. We can see them in other parts of the foreground arms, however, such as the region north of IC 2163 before the arms cross in front of the disk. There are many faint red stars in these parts too, alongside young clusters and other dust lanes.

The blue stars in the foreground spiral arms are interesting because of what they tell us about the processes by which density waves trigger or organize star formation. This is the first example in an external galaxy where we can see such triggered star formation in projection against a background source. We see at this resolution (1 pixel = 17 pc) blue stellar-like images mixed with the dust. These blue objects are probably young clusters (Paper V).

The star formation process looks normal at this perspective. The filaments contain clumps, and the clumps form stars. This is the same morphology as in local regions that are much smaller, such as Taurus. We cannot see any dust structure that might be indicative of cloud disruption, such as comet tails pointing away from the blue clusters, but the dust opacity may be too low for such detail on these scales.

The tidal forces acting on NGC 2207 are primarily perpendicular to its disk, and this galaxy is not flocculent, so it is unlikely that the parallel dust streamers in the spiral arm are from tidally stretched flocculent arms, as in IC 2163. The parallel dust filaments in NGC 2207 look similar to parallel dust filaments in the arms of M81. These M81 filaments are often at the upstream and downstream edges of the strings of giant H II regions in the arms, and they may be parts of dense shells (Kaufman, Elmegreen, & Bash 1989), but it is also possible that M81 and other grand-design spirals have the same multistranded shock structures in their arms as NGC 2207.

Not all of the spiral arms in NGC 2207 have parallel dust structure. In the west, midway out in the optical disk, the dust lanes cut through the arm like spurs, but farther to the west, in the outer arm, some of the dust lanes are parallel again. Perhaps this change to spurs marks an orbital resonance.

#### 5. THE DENSE DARK CLOUD AND STAR-FORMING REGION IN THE FAR WEST OF NGC 2207

There is a peculiar dust region that appears to be associated with star formation in the far western part of the outer spiral arm of NGC 2207. It is the site of an intense radio continuum source, as shown in Figure 4, and the most luminous  $H\alpha$  source in the system (see map in Paper V). An enlargement of the *HST* image is labeled feature *i* in Figure 6 below. In Paper III, we conjectured that this radio continuum source was a background radio galaxy, not associated with NGC 2207, because if it were at the distance of 35 Mpc its luminosity would be unlike anything else in either galaxy. Now, its coincidence with a dense dust cloud and bright young star cluster, and the similarity between the velocities of the associated  $H\alpha$  emission and the  $H\text{ I}$  emission from NGC 2207 in this vicinity, make the association of this radio continuum source with NGC 2207 more likely.

With a resolution of  $1''.0 \times 1''.9$  FWHM, Vila et al. (1990) detected a compact, radio continuum core with a deconvolved Gaussian size of  $\sim 1''$  (Fig. 4, *plus sign*) at the location of the star cluster, surrounded by a more extended radio component. The core has flux densities of  $S(20) = 3.4$  mJy at 20 cm and  $S(6) = 1.4$  mJy at 6 cm and a spectral index  $\alpha$  of  $-0.7$ . Integrating over a  $7''.5 = 1.3$  kpc region, they measured  $S(20) = 10.3$  mJy,  $S(6) = 3.4$  mJy, and  $\alpha = -0.9$ . The lower resolution radio continuum obser-

vations in Paper III found even more extended emission here, with  $S(20) = 22$  mJy and a deconvolved size of  $2.5$  kpc  $\times$   $2.2$  kpc (FWHM). Thus, the core has a radio continuum luminosity 300 times that of Cas A; the core plus extended component forms a large, nonthermal radio source with a radio continuum luminosity  $\sim 1500$  times that of Cas A if the spectral index of  $-0.9$  applies throughout (taking the 6 cm luminosity of Cas A as  $7 \times 10^{17}$  W  $\text{Hz}^{-1}$ , from Weiler et al. 1989). Although comparable in radio luminosity to the most luminous radio supernovae (e.g., SN 1986J, SN 1988Z; Van Dyk et al. 1993), the large linear size of the source in NGC 2207 suggests that it is something else.

The  $H\alpha$  source in this region has a luminosity (from Paper V) of  $1.4 \times 10^{40}$  ergs  $\text{s}^{-1}$  and a diameter of  $6''$ . Uncorrected for reddening, the  $H\alpha$  flux is equivalent to  $S(6) = 0.13$  mJy of optically thin free-free emission if  $T_e = 10^4$  K. This is much smaller than the measured 6 cm flux density from approximately the same region. Its  $H\alpha$  luminosity uncorrected for reddening is similar to that of 30 Dor (Kennicutt & Hodge 1986) and the brightest  $H\text{ II}$  region in M51 (van der Hulst et al. 1988). The strong nonthermal emission from the NGC 2207 source suggests that some of the  $H\alpha$  flux may be from shocks or synchrotron sources rather than photoionization. A significant amount of  $H\alpha$  could be occulted by the dark cloud, but not all of it, because we still see star clusters, and the radio continuum and  $H\alpha$  sources are larger than the cloud.

The structure of the region in the *HST* images is also peculiar because of a V-shaped feature, possibly a conical outflow, that has a bright star cluster at the apex and opens up to the north. This V shape seems to extend on its western side to a bright starlike object in the north-northwest

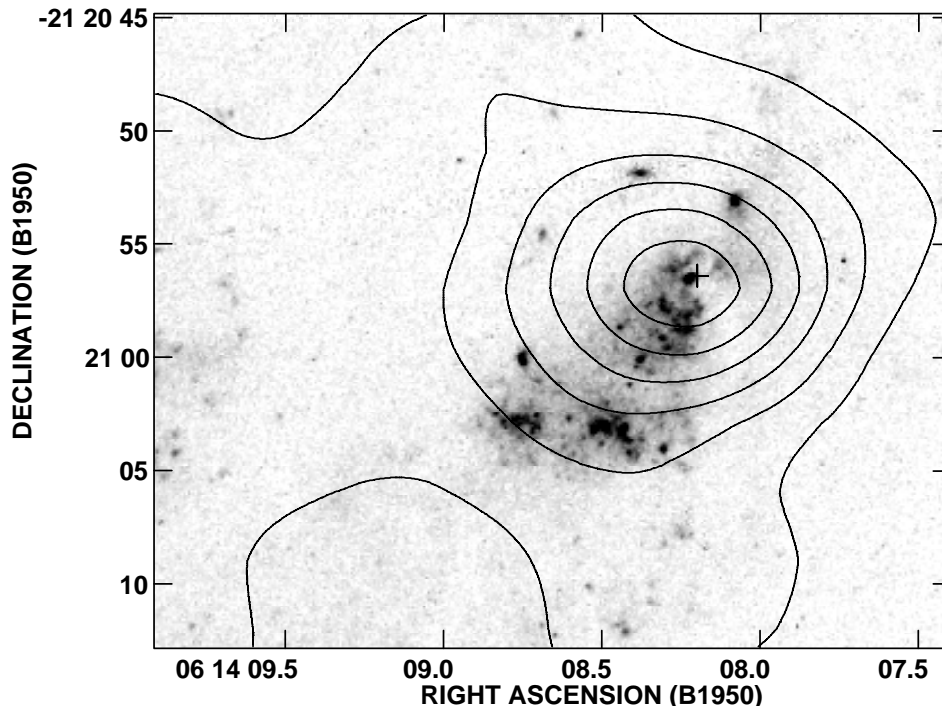


FIG. 4.—Enlargement of the region containing the nonthermal radio continuum source on the western arm of NGC 2207 (cf. feature *i* in Figs. 6 and 7). The contours are radio continuum emission at  $\lambda = 20$  cm with a resolution of  $10'' \times 6''.5$  (FWHM). They are overlaid on the *HST* *B*-band image in gray scale. The contour interval is 10 K, which is 3 times the rms noise, and the contour levels are at 1, 2, 3, 4, 5, and 6 times the contour interval. The plus sign marks the location of the radio continuum maximum in the higher resolution observations by Vila et al. (1990).



(which may not be related to it) at a distance of  $\sim 500$  pc from the central cluster. A dense dust cloud trails off in the other direction. If this V comes from a conical outflow, then there may be a peculiar and energetic star or collapsed object in this region, possibly with an accretion disk and jet. An X-ray survey might reveal a compact source.

To the southeast of the dense cloud and central star cluster, there are a number of smaller star clusters (Fig. 6i below) that appear to be distributed in concentric arcs  $\sim 400$  pc long. A similar pattern was found in an equally intense region of star formation in the galaxy NGC 6946 (Elmegreen, Efremov, & Larsen 2000a), where several cluster arcs are inside and at the edge of a cleared  $\sim 600$  pc cavity surrounding a  $\sim 15$  Myr old globular cluster. If these arcs are not optical illusions (e.g., Bhavsar & Ling 1988), then the clusters could have been triggered in expanding partial shells. The large scale of this process, the unusual morphology, and the strong nonthermal radio emission from the NGC 2207 source suggest peculiar conditions. Considering the arc sizes, the explosions that triggered the clusters would have been extremely energetic, more than just single supernovae, and they were possibly one-sided since the apparent cluster arcs are not complete circles. It may be that a few extremely massive stars and their hypernovae (Paczynski 1998) are involved, in which case there could have been a gamma-ray burst from these regions several tens of millions of years ago (see also Efremov 1999). The one-sided nature of the cluster distribution could also be the result of an initial gas concentration on that side.

There is no significant excess of H I gas at the location of this dust cloud and star-forming region (see Fig. 8 below). An H I cloud exists slightly to the south, along the spiral arm in a large darkish region, and another H I cloud is to the northeast, in the dark interarm region. These two clouds could be pieces of the envelope of a former giant molecular cloud centered on the dust feature. To the south along the same arm, the next big star-forming region does have a prominent H I cloud associated with it. Thus the more intense star-forming region associated with the dense dust cloud and the strong radio continuum source could have blown apart the low-density parts of its cloud. We will discuss the other H I structure in these galaxies in more detail in § 8.

The mass of the dust cloud can be estimated from its size ( $\sim 300$  pc  $\times$  140 pc) and apparent darkness. Paper V measured brightness deficits of  $\Delta m_V = 1.78 \pm 0.3$ ,  $\Delta m_B = 1.73 \pm 0.3$ ,  $\Delta m_V = 1.24 \pm 0.3$ , and  $\Delta m_I = 1.38 \pm 0.3$  mag in the dark cloud. Since these values are all about equal, the dark cloud is optically thick in even the I band. If we assume an average visual extinction of 3 mag (twice  $\Delta m_V$  because of foreground stars), then the mass would be  $\sim 10^6 M_\odot$ .

## 6. INNER DISK SPIRALS IN IC 2163

Paper III speculated that the nuclear region of IC 2163 might have a weak bar, or possibly be forming a bar now as the result of the interaction, as predicted by Noguchi (1987) and shown again by Gerin, Combes, & Athanassoula (1990) and Paper I. The *HST* image shows no evidence for such a bar, but there is a spiral arm system inside the oval that is elongated to make the overall structure resemble the inner Lindblad resonance (ILR) region of a bar.

The elongation of the two inner spirals arms is actually much more pronounced in the image than it is in reality because the galaxy is inclined with a line of nodes nearly

parallel to the *minor* axis. This is the opposite of what most galaxies have: usually the projection line of nodes is along the major axis. For IC 2163, the kinematic minor axis is approximately the same as the morphological major axis in the oval region (Paper III). The kinematic minor axis from H I velocities has a position angle of  $155^\circ$ , and the morphological major axis from optical and H I isophotes has a position angle of  $128^\circ$ , which is only  $27^\circ$  different. The inclination is  $30^\circ$ – $40^\circ$  from the model fits. Thus the bright oval in IC 2163 is actually more elongated than the image shows (cf. Fig. 2), by a factor of 1.2–1.3, and the spirals inside the oval are more circular.

Figure 5 displays the radial behavior of the arm-interarm contrast of the inner disk spirals in V and I bands. The arm contrast is nearly constant with radius, which is unusual for the inner parts of density-wave arms (Elmegreen & Elmegreen 1995).

There is a curious dynamical property of this interaction that may point to the origin of the inner disk spiral and even suggest a common mechanism for close interactions to trigger nuclear gas accretion and nuclear starbursts. This property follows from the relative position of the companion, NGC 2207, and the rotation curve inside IC 2163.

Figure 13 in Paper III showed the rotation curve of IC 2163, from the H I data. It is steeply rising as a solid body between the center and  $\sim 7''$ , and then it is more slowly rising in a steady fashion after that. This inner steep rise means that there will be an inner ILR somewhere inside  $7''$  and an outer ILR somewhere outside  $7''$  for any bisymmetric spiral pattern that has a sufficiently low pattern speed. The semiminor axis of the oval is about  $15''$  and the inner radius of the inner spiral is about  $5''$ . Thus, the inner spiral could extend between the inner and outer ILRs.

For a conventional bar potential with an ILR, there is a shock, or dust lane, parallel to the bar on the leading side and then a twist to a ring or inner spiral near the ILR (Athanassoula 1992). If there is both an outer ILR and an inner ILR, then there will often be a  $90^\circ$  turn of this shock between the two resonances (Sanders & Huntley 1976). The spiral inside the oval of IC 2163 turns about  $90^\circ$  and may

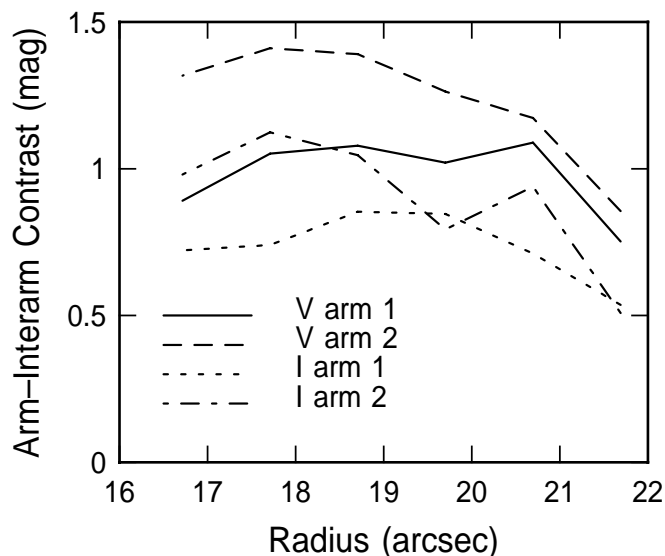


FIG. 5.—Arm-interarm contrast as a function of radius for the inner spirals in IC 2163. The lack of an increase with radius suggests a location inside the ILR.

have its outer radius at the outer ILR, which would then be at the inner extent of the oval. The spiral could have its inner radius at the inner ILR. The whole oval would then be showing the response of the galaxy IC 2163 to a barlike or  $\cos 2\theta$  potential: The long axis of the oval, which has an axial ratio of about 3:1 corrected for inclination, is along the “bar,” where the inward radial force and  $\cos 2\theta$  are maxima. The inner near-circular spiral, which extends from the inner minor axis of the “bar” to a smaller radius, twisting  $90^\circ$  along the way, would be the ILR shock feature. This barlike structure presumably gave IC 2163 the de Vaucouleurs type of SB(rs)c pec, even though there is no bar in the classical sense.

An interesting thing about this system is that the tidal potential from NGC 2207 has the correct orientation to contribute to the “bar” potential in IC 2163, along with the oval itself. The tidal force from NGC 2207 pinches inward on IC 2163 in a direction that is perpendicular to the line connecting the two galaxies, and it pulls outward on IC 2163 in a direction that is parallel to this intergalactic line. This makes a  $\cos 2\theta$  forcing, much like in a bar (Combes 1988). For a real bar, the perturbation in the inward direction, relative to a circular potential, is along the bar, and the perturbation in the outward direction, relative to a circular potential, is on the minor axis of the bar. Thus the inward tidal pinch and outward tidal pull from NGC 2207 make IC 2163 feel like it has a bar oriented in a direction perpendicular to the line connecting the two galaxies. This is in fact the mean orientation of the oval during the last  $\sim 80$  Myr, which is the total time from the current position  $\sim 40$  Myr after perigalacticon back to the symmetric position prior to perigalacticon. Recall that IC 2163 is quickly moving along the back side of NGC 2207 in a direction roughly from west to east and parallel to the disk of NGC 2207. The transient deformation of the disk into the oval accentuates this tidal force, increasing the barlike potential, and this transient bar can drive ILR spirals.

What makes the tidally induced bar potential so prominent in IC 2163 is the fortunate circumstance of catching the galaxy pair close to perigalacticon, and the extreme proximity of the encounter (perigalacticon was estimated to be  $\sim 2.3$  times the radius of IC 2163 in Paper IV). Presumably, the barlike response in IC 2163 will last only during the closest approach, unless IC 2163 actually forms a permanent bar during this time, which is possible (Paper I).

The corotation position of the barlike potential in this interpretation is the companion galaxy, NGC 2207. This is a large distance from IC 2163, and it gives a low pattern speed (approximately  $5.6 \text{ km s}^{-1} \text{ kpc}^{-1}$ ). For such a pattern speed, the inner and outer ILRs should both exist for the rotation curve of IC 2163, and they should be sufficiently well separated to account for the inner disk spiral structures. Unfortunately, the H I rotation curve is not sufficiently accurate, considering the streaming motions, to determine these inner and outer ILR positions any better.

A transient, tidally induced, barlike potential in an interacting galaxy should be able to drive mass inflow to the nucleus in much the same way as a permanent bar structure. The bar produces torques on the gas, and the gas moves to the center, primarily along the dust lanes and ILR spirals, with the resulting loss of angular momentum. If the encounter is too weak and fast to make a bar (the criteria for bar making were discussed in Paper I), then the system will end up with a starburst in the nucleus of one or both

galaxies (if they both felt an in-plane tidal force), and there will be no evident bar structures at late times to indicate how the gas got to the center so quickly. In this way, tidal interactions may trigger gas accretion and nuclear starbursts in a variety of seemingly mild encounters.

The inner disk spiral arms of IC 2163 may be an earlier form of the very bright inner disk spiral arms of NGC 5394, discussed in § 1. The model in Kaufman et al. (1999) finds that the latter developed from an ocular structure present at a slightly earlier time. NGC 5394 has a central starburst, and its inner disk spiral arms are unusual in that two of the three bright arms show no evidence of star formation.

## 7. PECULIAR EMISSION STRUCTURES

We examined the *HST* image in detail for all peculiar emission features that might be conical or jetlike. Several interesting candidates were found. Most have a size in the range from 100 to 1000 pc.

### 7.1. Features on 100 to 1000 pc Scales

A collection of peculiar emission features on 100 to 1000 pc scales is found in Figure 6, and a finding chart is given in Figure 7. North is up for all the images in Figure 6 and the physical scale is on the right, assuming a galaxy distance of 35 Mpc. No feature appears in only one filter, which would make it an image flaw.

There are several linear or arc-shaped structures of blue knotty emission, such as *c*, *h*, *s*, *t*, and *o*. They could be composed of young stars except for their peculiar linear shapes. Feature *f* is similar to these but brighter; *u* is a curved line of star formation. Features *a*, *g*, and *p* are other multiple-point structures, apparently made from young stars.

Jetlike features are seen in several places: *e* contains two jetlike structures that point toward each other; *q* has two jetlike features with a starlike object in the middle; *b* has a small jetlike object pointing away from a bright diffuse patch and other linear structures perpendicular to this; *g* (mentioned above) also contains a streak of faint emission between the central pointy structure and a starlike object in the north; *n* contains three faint linear emission streaks in what seems to be a region of star formation.

V-shaped features that could be conical emission regions include *i*, the strong radio continuum source in the far west of NGC 2207, containing intense star formation, a dense dust cloud, and a possible conical emission region in the north (see § 5); *l*, a sideways V shape, possibly a conical dust and reflection feature in the NGC 2207 spiral arm with blue star formation knots in it; and possibly *r*, a peculiar dark feature just to the upper right of the center, with a bright rim around it. Feature *j* contains two nearly parallel streaks running vertically in the figure; one streak is bright and the other is dark, giving it a three-dimensional quality.

There are two dust shells: *k*, a dust shell with three star formation knots in it, most likely in the NGC 2207 spiral because of the blue color of the star formation, and *m*, a dust shell with a red star in the middle (possibly a foreground star; see Paper V). To the northwest of the dust shell *k*, there is a bright kiloparsec-long arc (feature *d*) that looks like reflection off the inner edge of the dust lane that is inside the inner disk arm.

The reddish features (*k*, *d*, *l*, *m*, *n*) juxtaposed on top of IC 2163 could be inside IC 2163 or in the foreground spiral arms of NGC 2207. The other features are mostly white or

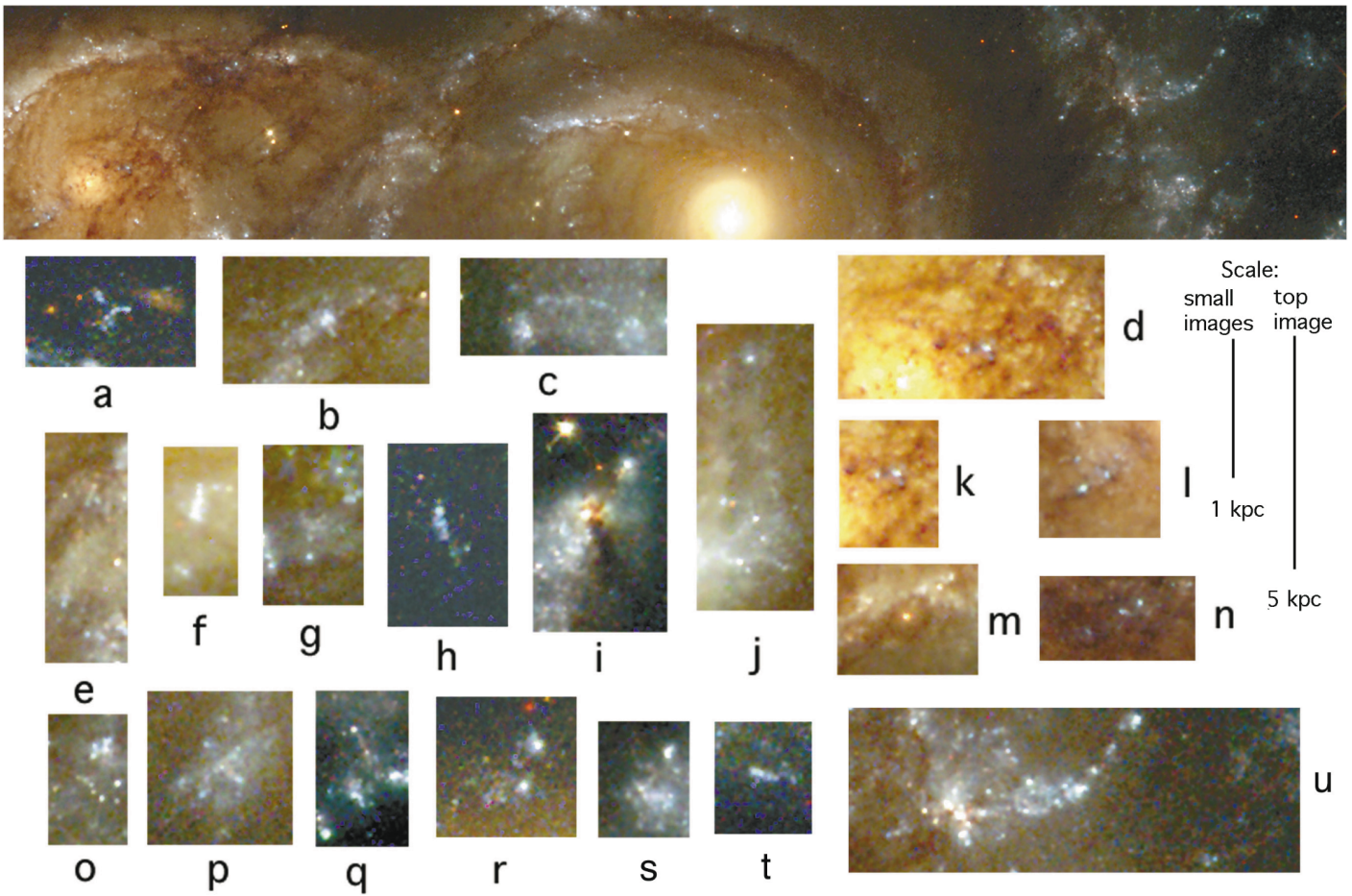


FIG. 6.—Montage of peculiar features showing linear or smooth emission structures. The physical scale on the right assumes a distance of 35 Mpc.

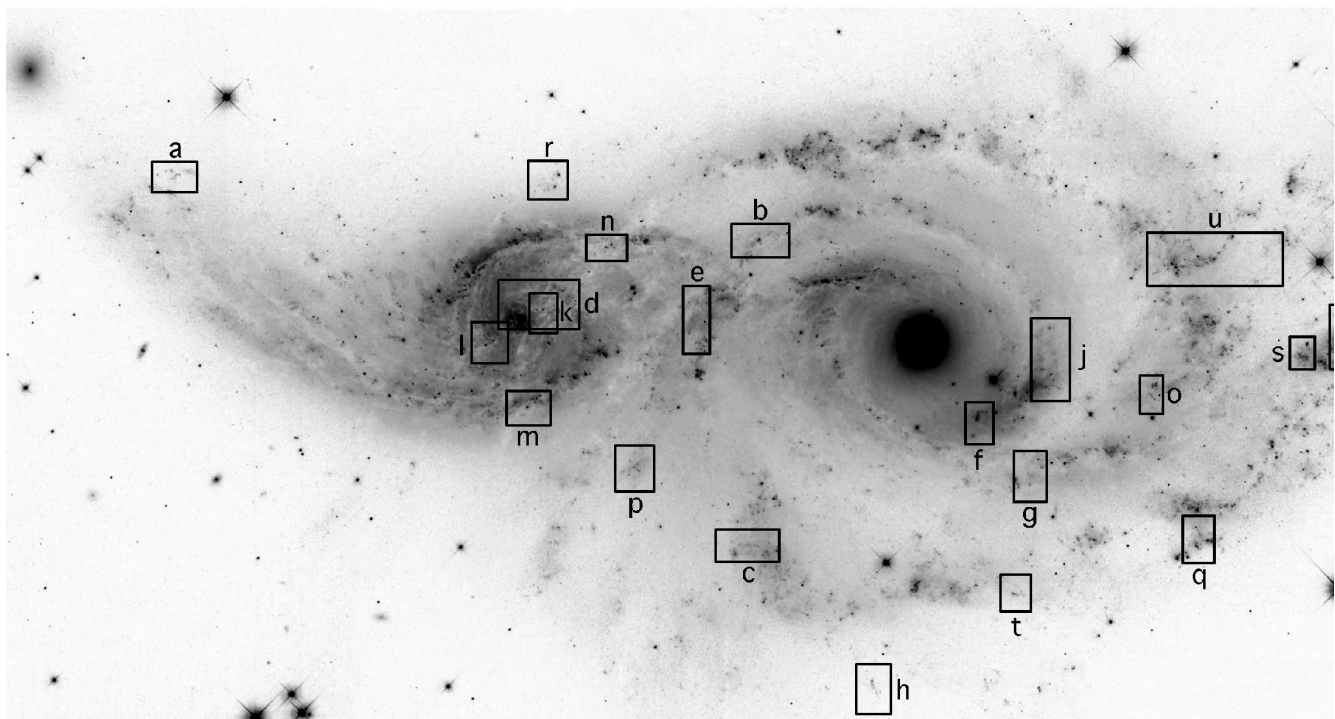


FIG. 7.—Finding chart for the peculiar features shown in Fig. 6

blue in color, and except for *a* and possibly *r*, are positioned to be likely members of NGC 2207.

Individual jetlike objects are typically 1"–2" or 150–300 pc long; the two streaks in feature *e* span 1000 pc. Analogous objects are not known in our Galaxy; much smaller versions of jets could be those associated with SS 443 (Margon 1984), the Crab Nebula jet (van den Bergh 1970; Gull & Fesen 1982), or Cas A (Fesen & Gunderson 1996). The jetlike regions in NGC 2207 might also be radio sources that are too weak and small to have been seen in our VLA survey. The origin of these features is not clear. Some may be related to mass transfer events in which gas from IC 2163 recently impacted the disk of NGC 2207, some may be optical illusions, and some may be normal galactic features not previously recognized in other galaxies.

### 7.2. Larger Scale Linear Features

The top panel of Figure 6 shows four unusual elongated features that lie on approximately the same line. Each cuts across a spiral arm at a large angle. The most prominent is the straight ridge of star formation along the innermost northern spiral arm of NGC 2207 (near the middle of this panel at  $\alpha = 6^{\text{h}}14^{\text{m}}15^{\text{s}}.7$ ,  $\delta = -21^{\circ}21'05''$ , B1950.0). This ridge alone is not so peculiar, because it has a dust lane on the inner edge and normal-looking young stars, but it is unusually straight for a density-wave feature, and it does not follow the curvature of the rest of the arm. Just to the west of this bright feature (and along the same line) is a faint, thinner emission streak composed of several diffuse spots with no obvious dust lane. It cuts across the same spiral arm. In the opposite direction, in the next outer arm of NGC 2207 to the east of the brightest linear streak, there is another linear feature composed of dust in the center of two streaks of star formation; this is also not aligned with its local arm. The fourth feature is in the middle western arm of NGC 2207, on the right side of the top panel at  $\alpha = 6^{\text{h}}14^{\text{m}}10^{\text{s}}.7$ ,  $\delta = -21^{\circ}20'47''$  (enlarged in Fig. 6*u*). The linear part crossing the spiral arm is made of dust and star formation, but just to the west of the arm, in the interarm region, is a large, diffuse "bubble-like" object. Several blue emission spots and a dust filament curve upward from the end of the bubble, and a faint, sideways V-shaped object that looks like a bow shock is farther to the west, along the same line (cf. feature *u* in Fig. 6). The whole line of four features points back to within 1" of the nucleus of IC 2163. This alignment resembles a jet, but there is no prominent radio continuum source in the center of IC 2163 or along the line. Paper III found a strong radio continuum ridge  $\sim 15''$  north of the line connecting these four linear features, and aligned at an angle of  $30^{\circ}$  relative to it.

The original WFPC2 chip seam on the mosaic runs underneath and almost parallel to this linear structure, beginning at the bright emission knot in the arm to the east of the main ridge and ending at the edge of the image on the west. However, the individual features are visible in the separate fields before the mosaic was made, so these features are not artifacts of the seam.

Detailed numerical models of both galaxies in the interaction (Struck et al. 2000) occasionally find linear features from debris trails with material pulled out of IC 2163 and brushing the back side of NGC 2207. The lifetimes of any linear features composed of stars and dust are constrained by galactic rotation to be fairly short, less than several million years.

## 8. H I EMISSION AND STAR FORMATION

Maps of the H I emission from each galaxy are shown superposed on the *HST* images in Figures 3 and 8. Two peculiarities of the H I emission are its large velocity dispersion ( $\sim 50 \text{ km s}^{-1}$ ) and large cloud masses ( $\sim 10^8 M_{\odot}$ ; Paper III), which are characteristic of interacting systems (Paper II; Kaufman et al. 1997, 1999; Irwin 1994; Hibbard 1995).

The largest clouds in these galaxies are not clearly associated with star formation. Figure 14 in Paper III is a finding chart for  $10^8 M_{\odot}$  clouds that were also outlined on the contour diagrams in Figures 8 and 16 of that paper. The same contours are shown here in Figures 3 and 8, but without the outlines for giant clouds. Here the clouds in NGC 2207 are identified by the notation N1, N2, and so on.

In IC 2163, there are five giant concentrations of H I: two in the eastern tidal arm, one in the streaming region of the eastern tidal arm to the north, one in the western tidal arm near the center of NGC 2207, and one in the northern eyelid region (cf. Fig. 3). None are associated with specific star formation regions, but the one on the northern eyelid has star formation all along its inside border. The one in the western tidal arm is heavily obscured by NGC 2207. There is a less massive H I cloud in the southern eyelid region, which is centered on a region with bright patches of star formation.

In NGC 2207 there is a giant H I cloud in the far northwest (N1) with only faint emission in the *B* band, and three more in the western spiral arm below this (N2, N3, N4) with bright star formation only in the lowest one. The other two giant clouds in NGC 2207 (N5, N6) are in the east in Figure 8, in the region that is foreground to IC 2163. One (N5) is at the end of the outer eastern arm of NGC 2207 and is associated with a dust feature and faint blue cluster (cf. Fig. 1). The other (N6) is in a region crossed by dust lanes between the tidal bridge of IC 2163 and the middle arm on the eastern side of NGC 2207. The cloud is not centered on a bright star-forming region. It coincides with part of a 10 kpc long, radio continuum ridge (see Paper III).

The bright star-forming regions are mostly associated with smaller H I clouds, having masses of  $10^7 M_{\odot}$  or less. At this level of H I emission, many star-forming regions have some H I nearby, as is often the case in noninteracting galaxies. For example, in NGC 2207, the small patches of star formation in the southern arm are all associated with these less massive H I clouds, as is the small patch south of feature *i* (Fig. 6) in the western arm. The middle arm on the western side of NGC 2207 winds around to the north and then crosses in front of the central part of IC 2163. In the north, this arm has several bright regions of star formation along the H I ridge, some of which coincide with H I clumps. On the eastern side, the arm, seen as the dust streamers discussed in § 4.3, also coincides with the H I ridge.

The giant star-forming region (feature *i*) that is associated with the intense radio continuum source on the outer western arm has no H I cloud, although there are smaller clouds to the south and west of it (N3, N2). The dense dust in this region suggests that the hydrogen is present in molecular form.

There is no direct optical evidence for the large H I velocity dispersions that are present in these galaxies, which is typically  $30\text{--}50 \text{ km s}^{-1}$  (Paper II). Such motions would be supersonic for H I. Large random motions also imply that

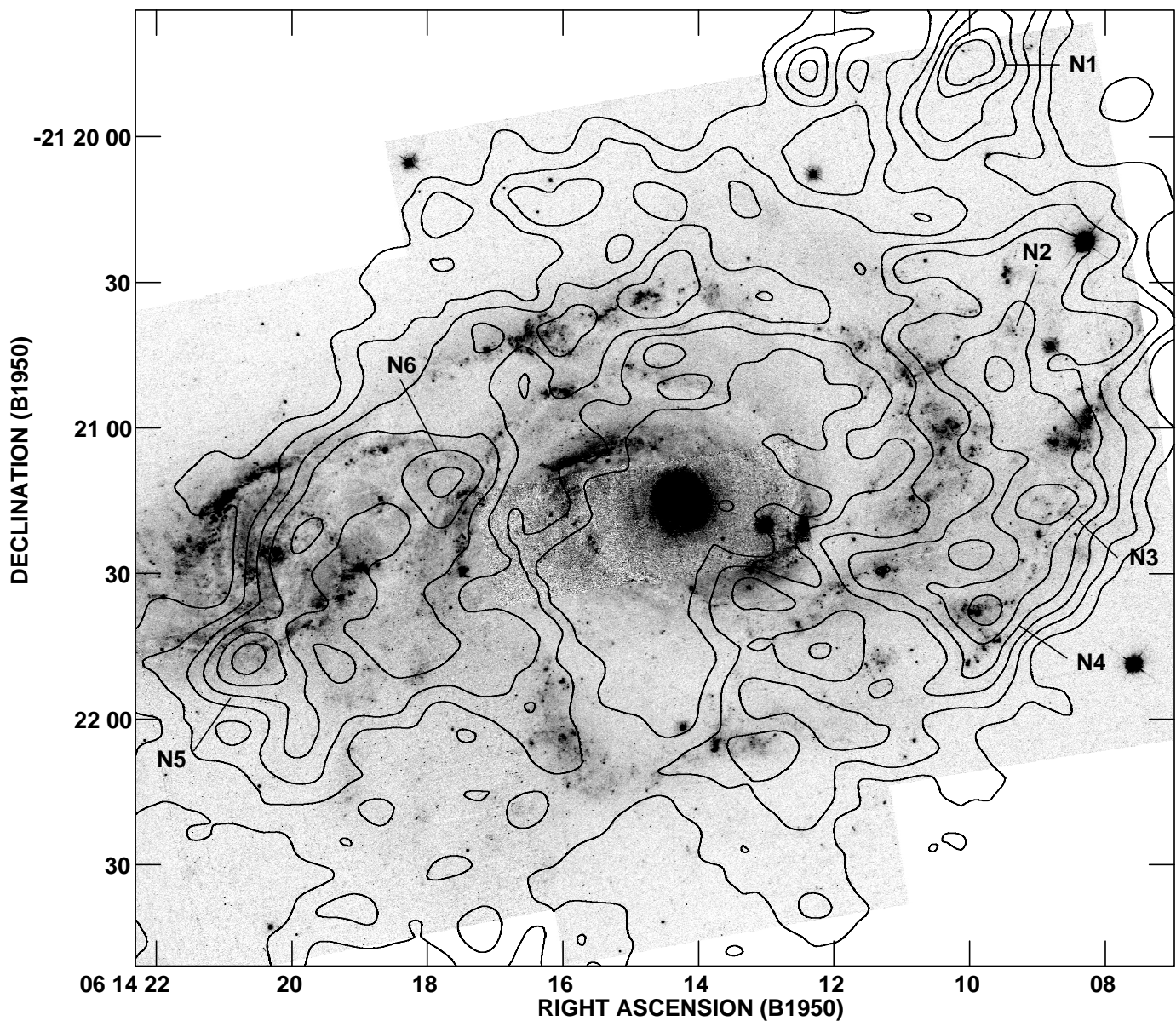


FIG. 8.—H I column density contours of NGC 2207 (from Paper III) with a resolution of  $13''.5 \times 12''$  (FWHM) overlaid on the *HST* *B*-band image in gray scale. Contour levels of the line-of-sight H I column density are 10, 15, 20, 25, 30, and  $35 M_{\odot} \text{pc}^{-2}$ . The dust streamers in the backlit spiral arm of NGC 2207 are discussed in § 4.3 and lie along an H I ridge.

the gas disks are thicker than normal, by perhaps a factor of  $\sim 5$ . The models in Paper IV predict a warp in NGC 2207 that is pointed away from us on the IC 2163 side and toward us on the western side. Paper III found that on the western side of NGC 2207, the optical radial surface brightness profile has a plateau from  $40''$  to  $90''$ , which corresponds to the broad ring of H I emission that peaks at  $70''$ . The increase in the line-of-sight thickness produced by the warp may be responsible for the prominence of the H I ring on the eastern and western sides and for the unusual behavior of the radial surface brightness profile in the optical on the western side. Since most of the massive clouds in NGC 2207 are in these directions, their surface mass densities would be slightly smaller than computed by neglecting the warp.

The high H I velocity dispersion could affect the optical observations in other ways too. The dispersion could

broaden the gas response to the spiral arms, for example, or remove the tendency for the gas to shock once in a thin dust lane. Instead, it could be shocking several times in the parallel dust lanes that are observed in front of IC 2163 (see § 4.3). The H I line profiles are typically not Gaussian, so they could be composed of a small number of streams with different velocities. In that case, the high velocity dispersion could result from variations in the systematic motions within the H I synthesized beam. These systematic motions could lead to the multiple shocks seen as dust lanes. Because the H I observations have a large beam ( $13''.5 \times 12''$ ), any streaming motions on a kiloparsec scale would be unresolved and appear only as turbulence.

Strong turbulence or high-speed streaming motions could also make the arms in NGC 2207 thicker than those in other spiral galaxies, such as M100 and M81. The NGC 2207 arms are similar to those in luminosity class III gal-

axies, which are usually much smaller than NGC 2207 (Iye & Kodaira 1976). This makes sense if the relative thickness of the arms scales with the ratio of the velocity dispersion to the orbit speed.

The origin of the high H I velocity dispersion is not known. Other strongly interacting galaxies have these motions too, so the turbulence could come from internal adjustments to tidal forces. We show in Paper V that the regions of highest dispersion contain super-star clusters, so there could be a connection with star formation too.

## 9. CONCLUSIONS

The galaxies IC 2163 and NGC 2207 are involved in a near-encounter that has compressed IC 2163 in the plane and warped NGC 2207 out of the plane. Optical observations with *HST* show many interesting and peculiar features. Two types of extinction patterns were discussed in § 4: long parallel filaments in the tidal tail of IC 2163, and clumpy filaments in the spiral arms of NGC 2207 that are seen in projection against IC 2163.

The tidal tail filaments seem to be normal flocculent spiral arms that were in the disk of IC 2163 before the encounter and then got stretched out into the tidal tail after the encounter by the overall disk deformation. A numerical simulation reproduced these filaments well. The extreme youth of the interaction ( $\sim 40$  Myr) explains why the spiral arms were not individually affected much, except for the overall distortion that followed the tidal flow. Many of the filaments have star formation that trails systematically behind them, suggesting a large-scale acceleration of the gas relative to the stars that form inside it.

The foreground spiral arm in NGC 2207 shows multiple parallel filaments as well, but probably for a different reason. There could be multiple shocks in the density wave, or independent filaments that came in from the interarm region. Such structure could be normal for galaxies but not commonly observed because of the rarity of background lighting. In any case, star formation occurs in the clumps of these filaments in a way that resembles local star formation in small filamentary dark clouds. The process of star formation in the density waves of NGC 2207 is therefore one in which filaments, either made by the wave or preexisting, collapse gravitationally into globules, which then continue to collapse into clusters and individual stars. The star formation does not look like it is occurring at the interfaces between colliding clouds or colliding filaments.

Another interesting region is a dense dark cloud in a region of star formation on the outer western arm of NGC 2207. This is the site of the most luminous H $\alpha$  source in the galaxies, and a large, nonthermal radio continuum source

1500 times more luminous than Cas A. There is a massive cluster in the center, a conical feature like an outflow to the north, and other clusters in the southeast that could have been triggered by energetic explosions.

The spirals inside the oval of IC 2163 were discussed in § 6. The dynamical time of this inner region is much shorter than the interaction time, so these spirals could be part of the response. We suggested, on the basis of the rotation curve, that the central spirals could extend from the outer ILR to the inner ILR for a pattern speed that places corotation at the companion. In that case, the whole oval may be viewed as a barlike, stellar and gaseous flow pattern in the transient  $\cos 2\theta$  potential of the tidal field. The inner spirals are then a normal resonance response for such a bar. This circumstance highlights the interesting possibility that transient tidal forces may trigger nuclear gas inflow via barlike hydrodynamics even when there is no bar. It also suggests that postencounter starburst systems without obvious bars today may have had their major accretion events close to perigalacticon, when the orbits were highly distorted.

Numerous peculiar emission features were found after a close examination of the *HST* image. Many are linear with either smooth or clumpy internal structures, and some have starlike objects at one or both ends. They are typically several hundred parsecs long, although smaller features would be difficult to see. Some could be jets or conical outflows, but they are much larger than protostellar jets found in the Milky Way. They may be coincidental alignments of stars or clusters, but the smoothest ones do not look like this. A long line of four colinear features that are at odd angles to their local spiral arms was also noted.

The H I is weakly associated with star formation in these galaxies, but the largest H I clouds, with masses of around  $10^8 M_{\odot}$ , are not generally producing rich clusters. The H I velocity dispersion is 5 times higher than normal, which may explain why the spiral arms in NGC 2207 look thick and feathery.

The high-resolution images obtained by the *Hubble Space Telescope* have presented us with an unprecedented opportunity to study the morphology of a pair of interacting galaxies in the early stages of interaction. It has shown us detailed features not previously observed elsewhere and given us important insights into the early stages of galaxy interactions.

This work was supported by NASA through grant GO-06483-95A from the Space Telescope Science Institute. Support for the Hubble Heritage Team's contribution also came from STScI.

## REFERENCES

- Athanassoula, E. 1992, MNRAS, 259, 345  
 Berlind, A. A., Quillen, A. C., Pogge, R. W., & Sellgren, K. 1997, AJ, 114, 107  
 Bhavsar, S. P., & Ling, E. N. 1988, PASP, 100, 1314  
 Block, D. L., Elmegreen, B. G., Stockton, A., & Sauvage, M. 1997, ApJ, 486, L95  
 Combes, F. 1988, in Galactic and Extragalactic Star Formation, ed. R. E. Pudritz & M. Fich (NATO ASI Ser. C, 232) (Dordrecht: Reidel), 475  
 Combes, F., & Gerin, M. 1985, A&A, 150, 327  
 Donner, K. J., Engström, S., & Sundelius, B. 1991, A&A, 252, 571  
 Efremov, Yu. N. 1999, Astron. Lett., 25, 74  
 Elmegreen, B. G. 1988, ApJ, 326, 616  
 Elmegreen, B. G., Efremov, Yu. N., & Larsen, S. 2000a, ApJ, 535, 748  
 Elmegreen, B. G., et al. 1998, ApJ, 503, L119  
 Elmegreen, B. G., Kaufman, M., & Thomasson, M. 1993, ApJ, 412, 90 (Paper II)  
 Elmegreen, B. G., Sundin, M., Kaufman, M., Brinks, E., & Elmegreen, D. M. 1995a, ApJ, 453, 139 (Paper IV)  
 Elmegreen, B. G., & Thomasson, M. 1993, A&A, 272, 37  
 Elmegreen, D. M., & Elmegreen, B. G. 1995, ApJ, 445, 591  
 Elmegreen, D. M., Kaufman, M., Brinks, E., Elmegreen, B. G., & Sundin, M. 1995b, ApJ, 453, 100 (Paper III)  
 Elmegreen, D. M., Kaufman, M., Elmegreen, B. G., Brinks, E., Struck, C., Klarić, M., & Thomasson, M. 2000b, in preparation (Paper V)  
 Elmegreen, D. M., Sundin, M., Elmegreen, B., & Sundelius, B. 1991, A&A, 244, 52 (Paper I)  
 Fesen, R. A., & Gunderson, K. S. 1996, ApJ, 470, 967  
 Gerin, M., Combes, F., & Athanassoula, E. 1990, A&A, 230, 37

- Gull, T. R., & Fesen, R. A. 1982, *ApJ*, 260, L75  
Hibbard, J. E. 1995, Ph.D. thesis, Columbia Univ.  
Irwin, J. A. 1994, *ApJ*, 429, 618  
Iye, M., & Kodaira, K. 1976, *PASJ*, 28, 415  
Kaufman, M., Brinks, E., Elmegreen, B. G., Elmegreen, D. M., Klarić, M., Struck, C., Thomasson, M., & Vogel, S. 1999, *AJ*, 118, 1577  
Kaufman, M., Brinks, E., Elmegreen, D. M., Thomasson, M., Elmegreen, B. G., Struck, C., & Klarić, M. 1997, *AJ*, 114, 2323  
Kaufman, M., Elmegreen, D. M., & Bash, F. N. 1989, *ApJ*, 345, 697  
Kennicutt, R. C., Jr., & Hodge, P. W. 1986, *ApJ*, 306, 130  
Low, F. J., et al. 1984, *ApJ*, 278, L19  
Margon, B. 1984, *ARA&A*, 22, 507  
Noguchi, M. 1987, *MNRAS*, 228, 635  
Paczyński, B. 1998, *ApJ*, 494, L45  
Roberts, W. W. 1969, *ApJ*, 158, 123  
Roberts, W. W., Jr., & Stewart, G. R. 1987, *ApJ*, 314, 10  
Sanders, R. H., & Huntley, J. M. 1976, *ApJ*, 209, 53  
Struck, C. 1997, *ApJS*, 113, 269  
Struck, C., et al. 2000, in preparation  
Sundin, M. 1989, in *Dynamics of Astrophysical Disks*, ed. J. A. Sellwood (Cambridge: Cambridge Univ. Press), 215  
van den Bergh, S. 1970, *ApJ*, 160, L27  
van der Hulst, J. M., Kennicutt, R. C., Crane, P. C., & Rots, A. H. 1988, *A&A*, 195, 38  
Van Dyk, S. D., Weiler, K. W., Sramek, R. A., & Panagia, N. 1993, *ApJ*, 419, L69  
Vila, M. B., Pedlar, A., Davies, R. D., Hummel, E., & Axon, D. J. 1990, *MNRAS*, 242, 379  
Weiler, K. W., Panagia, N., Sramek, R. A., van der Hulst, J. M., Roberts, M. S., & Nguyen, L. 1989, *ApJ*, 336, 421

ERRATUM: “HUBBLE SPACE TELESCOPE OBSERVATIONS OF THE INTERACTING GALAXIES  
NGC 2207 AND IC 2163” [ASTRON. J. 120, 630 (2000)]

BRUCE G. ELMEGREEN  
IBM Research Division

MICHELE KAUFMAN  
Departments of Physics and Astronomy, Ohio State University

CURTIS STRUCK  
Department of Physics and Astronomy, Iowa State University

DEBRA MELOY ELMEGREEN  
Department of Physics and Astronomy, Vassar College

ELIAS BRINKS  
Departamento de Astronomía, Universidad de Guanajuato

MAGNUS THOMASSON  
Onsala Space Observatory

MARIO KLARIĆ  
Columbia, SC

AND

ZOLT LEVAY, JAYANNE ENGLISH, L. M. FRATTARE, HOWARD E. BOND,  
C. A. CHRISTIAN, F. HAMILTON, AND K. NOLL

Space Telescope Science Institute

Received 2000 September 25; accepted 2000 September 25

Figure 7 was incompletely printed. The correct figure is shown below.

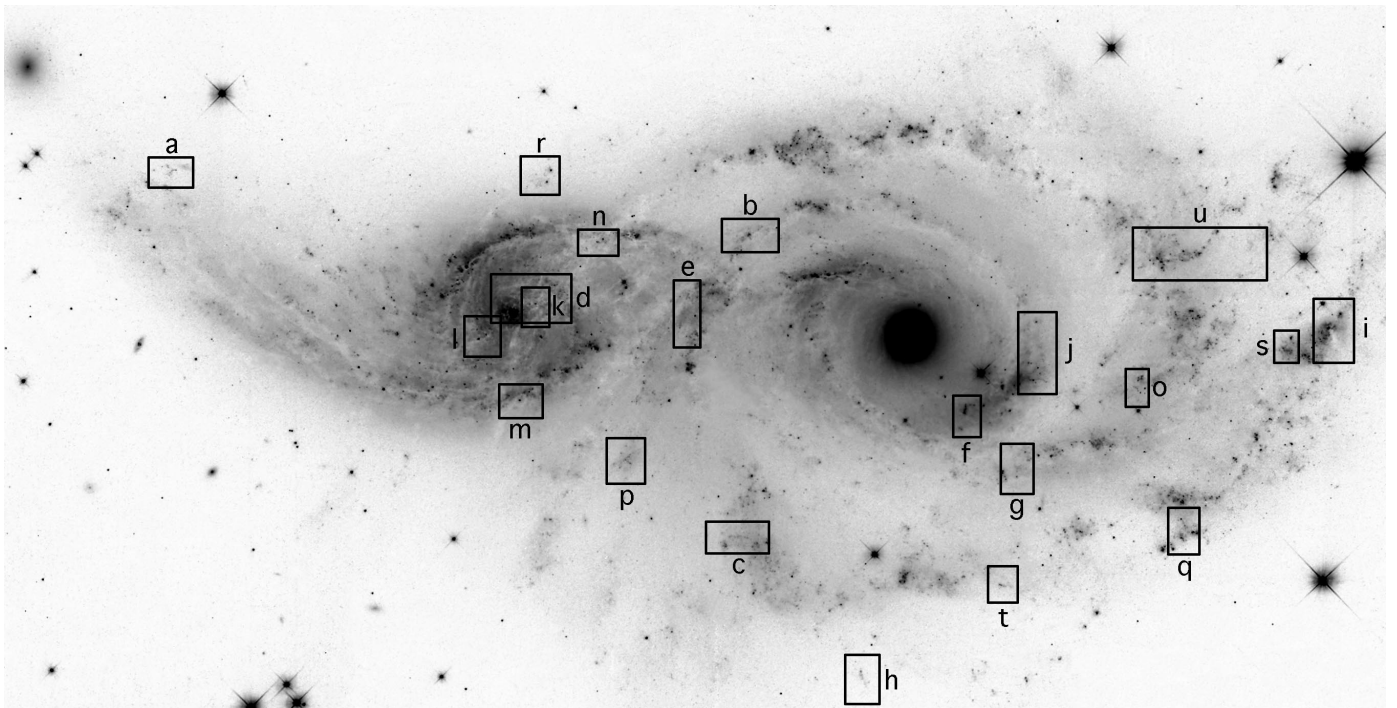


FIG. 7.—Finding chart for the peculiar features shown in Fig. 6